Volume 5, Number 5 (October 2012) p. 596-626 • ISSN 1983-4195
REVISTA IBRACON DE ESTRUTURAS E MATERIAIS
IBRACON STRUCTURES AND MATERIALS JOURNAL

Reforço à flexão de vigas de concreto armado com Tecido de Polímero Reforçado com Fibras de Carbono (PRFC) aderido a substrato de transição constituído por compósito cimentício de alto desempenho

Flexural strengthening of reinforced concrete beams with carbon fibers reinforced polymer (CFRP) sheet bonded to a transition layer of high performance cement-based composite


V. J. FERRARI [a]
vladimirjf@hotmail.com

J. B. DE HANAI [b]
jbhanai@sc.usp.br

Abstract

Resistance to corrosion, high tensile strength, low weight, easiness and rapidity of application, are characteristics that have contributed to the spread of the strengthening technique characterized by bonding of carbon fibers reinforced polymer (CFRP). This research aimed to develop an innovate strengthening method for RC beams, based on a high performance cement-based composite of steel fibers (macro + microfibers) to be applied as a transition layer. The purpose of this transition layer is better control the cracking of concrete and detain or even avoid premature debonding of strengthening. A preliminary study in short beams molded with steel fibers and strengthened with CFRP sheet, was carried out where was verified that the conception of the transition layer is valid. Tests were developed to get a cement-based composite with adequate characteristics to constitute the layer transition. Results showed the possibility to develop a high performance material with a pseudo strain-hardening behavior, high strength and fracture toughness. The application of the strengthening on the transition layer surface had significantly to improve the performance levels of the strengthened beam. It summary, it was proven the efficiency of the new strengthening technique, and much information can be used as criteria of projects for repaired and strengthened structures.

Keywords: strengthening of beams; carbon fibers; steel fibers concrete; fracture mechanic; rehabilitation of structures.

Resumo

Resistência à corrosão, elevada resistência à tração, baixo peso, facilidade e rapidez de aplicação, são algumas das características interessantes que têm contribuído para a disseminação da técnica de reforço caracterizada pela colagem de polímeros reforçados com fibras de carbono (PRFC) em elementos estruturais de concreto. Nesta pesquisa propõe-se uma inovação construtiva fundamentada no desenvolvimento de um compósito de alto desempenho à base de cimento Portland e fibras de aço (macro + microfibras), destinado a constituir o que está sendo preliminarmente chamado de "substrato de transição". A finalidade desse substrato é controlar melhor a fissuração do concreto da viga e retardar ou até evitar o desprendimento prematuro do reforço polimérico. Foram realizados ensaios específicos visando à obtenção de um compósito cimentício com características apropriadas para constituir o substrato de transição. Os resultados e as análises efetuadas mostram que foi possível desenvolver um material de elevado desempenho, traduzido por um comportamento de pseudo-encruamento, com elevados ganhos de resistência e tenacidade ao fraturamento. A aplicação do reforço com manta sobre a superfície do substrato de transição, formado a partir da reconstituição do banzo tracionado da viga com o compósito cimentício que foi desenvolvido, mostrou melhorar significativamente os níveis de desempenho da peça reforçada. Comprovou-se a eficiência da técnica de reforço proposta, além de reunir uma série de informações que podem ser exploradas para se tornarem úteis como critérios de projeto de estruturas recuperadas e reforçadas.

Palavras-chave: reforço de vigas; fibras de carbono; concreto com fibras de aço; Mecânica da Fratura; reabilitação de estruturas.

[a] *Universidade Estadual de Maringá, Departamento de Engenharia Civil, vladimirjf@hotmail.com, Avenida Colombo, 5790, Maringá-PR, Brasil;*
[b] *Universidade de São Paulo, Departamento de Estruturas, Escola de Engenharia de São Carlos, jbhanai@sc.usp.br, São Carlos, Brasil.*

Received: 04 May 2012 • Accepted: 03 Jul 2012 • Available Online: 02 Oct 2012

1. Introduction

In recent years, aspects related to durability, maintenance, retrofitting and strengthening of structures have been highlighted in the national scenario. Buildings with useful life below expectations, ageing of large structures, which already operate within the limits of stability and security (some of our bridges and viaducts, for example), and the lack of periodic inspections and preventive maintenances are factors which compete for the relevance of concepts related to strengthening and retrofitting of structures.

A retrofitted and/or strengthened structure must present performance higher than the presented before the intervention. In this way, the development of new technologies and techniques, more secure and efficient, arouse attention of researchers in various fields.

As a technique to strengthen structures of reinforced concrete, the application of CFRP is interesting, and has being accepted, owing the advantages, notably those related to the high resistance/weight ratio, immunity to corrosion, facility and rapidity of application. In Brazil, large structures have already been strengthened with CFRP. However, the already existing knowledge can be better conceived with a view to potentiating this technology.

Thus, the present paper intended to, as a construction innovation, develop a technique of flexural strengthening of RC beams, comprised of a process of previous retrofitting of the structure, by elaborating and applying a composite of high performance based on Portland cement and short steel fibers, intended to construct a so-called transition layer. With this layer, as shown in Figure [1], it is expected to reconstruct the tension zone of the RC beams in order to better explore the properties of resistance of strengthening with sheets of CFRP and, possibly, to enhance the beam performance as a whole.

It is known (Bian & Maalej [1], Ferrari [2], Leung [3]) that the strengthening of RC beams with CFRP sheets is susceptible to the appearance of a fragile, premature and extremely undesirable failure, because it prevents the total use of the strength properties to the polymer tensile.

Such form of failure anticipates the collapse of the strengthened beam by failure in the mechanisms of stress transfer. One of these mechanisms concerns to the localized debonding of strengthening (designated in the literature as peeling off), from its anchoring zone or zones with excessive concentration of flexural and/or shearing cracks. More significant increments of resistance only can be achieved if the premature forms of failure were prevented (FIB [4]).

Thus, with the proposed and presented in the study, it is imagined to withdraw a part of tensile zone of beams to be strengthened (frequently damaged by mechanical action, corrosion, natural wearing), as illustrates Figure [2], in order to reconstruct it with a high performance cement-based composite. For this purpose, it is assumed that the retrofitted part will form a transition layer, whose characteristics would be more appropriate for the application of the flexural strengthening with CFRP sheet.

2. High performance cement-based composite

In this section, are presented the experimental methodology and the results obtained in the development of a cement-based composite with characteristics more appropriate to reconstruct the tensile zones of RC beams, also serving as substrate to bond the CFRP. It is expected, with this composite, to constitute the transition layer in order to control better the cracking of concrete and to delay the premature debonding of the polymeric strengthening.

According to Ferrari [5], the modifications resulting from the addition of steel fibers to concrete, at relatively low rates (a maximum of 2%), are restricted only to the post-peak stage of the loading history. According to Ferreira [6], under such conditions, the steel fibers are not sufficient to inhibit the matrix cracking process which precedes the maximum load (subcritical growth of crack).

Thus, aiming to improve the cement-based composite behavior during the pre-peak stage of resistance, it is studied the effect of incorporating steel microfibers into conventional steel fibers, in an attempt to modify the composite in its microstructure and consequently to improve the process of stress transfer from matrix to fibers.

Figure 1 – Scheme of strengthening with CFRP sheets and transition layer

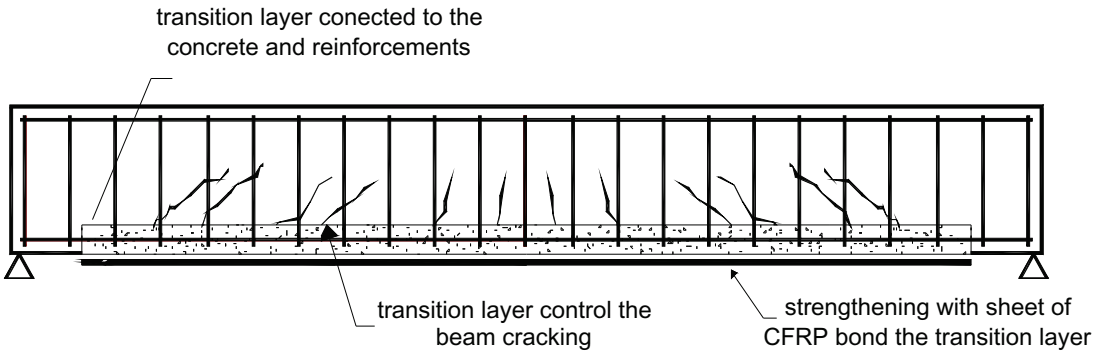

Figure 2 – RC beams with tensile zone damaged by effect of corrosion (Ferrari (5))

2.1 Test setup

In order to evaluate the behavior to bending tensile of cement-based composite it was performed bending tests on three points in prismatic specimens with central notch as recommended by (RILEM [7]). In the Figure 3 it is possible to observe the general aspect of the test setup. The tests were conducted by controlling the crack mouth opening displacement (CMOD), by using for this purpose a clip gauge.

2.2. Composites analyzed

It was analyzed a set of thirteen distinct composites formed from the variation in volume and type of steel fibers. They were divided into groups formed by three prisms (150 mm x 150 mm x 500 mm) molded with the same characteristics.
In the Table 1 are presented the different composites analyzed. These were divided into two steps according to the type of cement

Figure 3 – General setup of the flexural test on three points

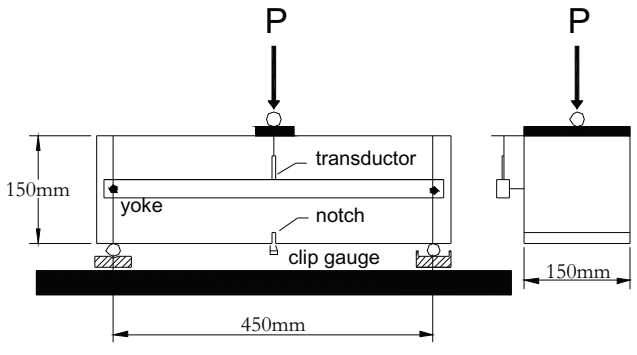

matrix used, mortar and microconcrete. The steel fiber specified here as "A", with trade name FS8-Wirand, was provided by the company Maccaferri – Latin America, has length of 25 mm with hooks at the ends and a diameter of 0.75 mm. As for the fiber "C", provided by the same manufacturer has a length of only 13 mm, hooks at the ends and a diameter of 0.75 mm.

2.3. Results of flexural tests on three points

2.3.1 Loads and resistances

In order to determine the flexional toughness of the composites, it was followed the recommendations prescribed by the work group (RILEM [7]). In the Table 2 are presented the values of loads and resistance calculated based on these recommendations.
For mortar composites, the addition of fibers constantly increased the value of resistance ($f_{fct,L}$) thus, for these composites the matrix contribution in terms of resistance was increased with the incorporation of steel fibers. The hybrid composites with addition of steel microfibers of type C to the fibers type A, were those with higher values of resistance ($f_{fct,L}$) among all the composite cement-based of mortar analyzed.
Regarding the composite cement-based of microconcrete, the resistance value ($f_{fct,L}$) for the composite CPM1A decreased in relation to the composite CPM. This showed that the isolated presence of fiber A does not improve the contribution of the micro concrete matrix regarding the resistance. However, with the incorporation of steel microfibers into fibers type A, it was verified an increase in the resistance value $f_{fct,L}$. This tendency was verified for the composites CPM1A1C and CPM1A2C, in which, the resistance was respectively, 28% and 37% higher than the CPM.
The values of resistances $f_{eq,2}$ and $f_{eq,3}$, characterize the composites behavior in relation to the fibers performance. In addition, it is highlighted among the composite cement-based of mortar, the performance of the composites CPA1.5A, CPA2A, CPA1.5A0.5C, CPA1.5A1.5C and CPA1.5A2.5C and, among the microconcrete composite cement-based, only the composite CPM1A2C. In these composites, the action of steel fibers has increased the level of the

Table 1 – Composites analyzed

Matrix	Group	Composites	Fiber volume	Fiber type	Age (days)	E_{cs} (MPa)
Mortar (A)	1	CPA	0%	-	29	23.839
	2	CPA1A	1%	A	29	22.696
	3	CPA1.5A	1.5%	A	29	23.100
	4	CPA2A	2%	A	29	23.974
	5	CPA1.5A0.5C	1.5%+0.5%	A+C	28	28.217
	6	CPA1.5A1.5C	1.5%+1.5%	A+C	28	32.261
	7	CPA1.5A2.5C	1,5%+2.5%	A+C	28	31.041
	8	CPA1.5A3.5C	1.5%+3.5%	A+C	28	29.137
Microconcrete (M)	9	CPM	0%	-	28	35.160
	10	CPM1A	1%	A	28	30.551
	11	CPM1A1C	1%+1%	A+C	28	26.281
	12	CPM1A2C	1%+2%	A+C	28	29.974
	13	CPM1A2.5C	1%+2.5%	A+C	28	19.900

a) Mortar composites: cement CP-V ARI PLUS:sand:water/cement – 1:3.0:0.5.
b) Microconcrete composites: cement CP-V ARI PLUS:sand:gravel 0:water/cement – 1:2.13:1.83:0.48.
c) Mortar composites cement consumption: 512kg/m^3.
d) Microconcrete composites cement consumption: 446kg/m^3.

Table 2 – Load and resistance according to RILEM (4)

Composite	Loads (kN)					Resistances (MPa)			
	F_L	F_M	$F_{R,1}$	$F_{R,4}$	$f_{fct,L}$	$f_{eq,2}$	$f_{eq,3}$	$f_{R,1}$	$f_{R,4}$
CPA	8.00	8.00	1.26	-	2.33	-	-	0.37	-
CPA1A	13.41	13.41	12.46	5.22	3.87	3.31	2.58	3.60	1.51
CPA1.5[a]	13.15	16.10	16.01	6.10	3.73	4.58	3.16	4.54	1.73
CPA2A	14.50	17.59	17.35	7.59	4.56	5.53	4.20	5.45	2.38
CPA1.5A0.5C	16.41	17.78	17.23	9.32	4.58	4.94	3.98	4.79	2.61
CPA1.5A1.5C	16.01	20.95	20.91	9.42	4.79	6.46	4.80	6.25	2.81
CPA1.5A2.5C	22.12	23.68	23.49	12.79	6.13	6.49	4.97	6.51	3.55
CPA1.5A3.5C	20.03	21.42	20.79	6.08	5.52	5.66	3.75	5.73	1.68
CPM	14.19	14.19	1.25	-	4.04	-	-	0.36	-
CPM1A	12.05	12.05	7.53	3.69	3.32	1.97	1.58	2.07	1.02
CPM1A1C	17.63	18.53	16.92	7.47	5.17	5.06	3.73	4.96	2.19
CPM1A2C	19.37	21.94	19.73	8.04	5.54	5.73	4.13	5.65	2.30
CPM1A2.5C	10.03	10.03	6.34	2.26	2.95	1.54	1.07	1.86	0.66

F_L – highest value of the load in the interval (CMOD) of 0.05 mm;
F_M – maximum load of composite;
$F_{R,1}$ e $F_{R,4}$ – residual loads corresponding to the deflections δ_{R1} = 0.46 mm and δ_{R4} = 3.00 mm;
$f_{fct,L}$- stress corresponding to F_L;
$f_{eq,2}$ e $f_{eq,3}$ – equivalente flexural tensile strengths;
$f_{R,1}$ e $f_{R,4}$ – residual flexural tensile strengths.

Figure 4 –P-CMOD curves of cement-based composites

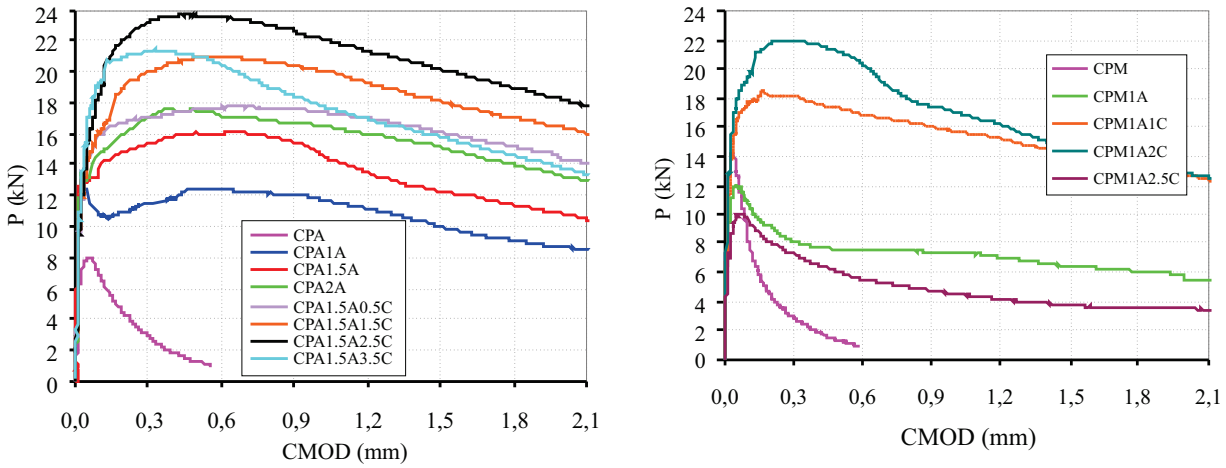

material resistance so that the equivalent flexional strength ($f_{eq,2}$) exceeded the resistance value given by the contribution of the matrix ($f_{fct,L}$) only.

2.3.2 P-CMOD Curves

In order to represent every composite behavior, it was selected among three curves obtained per group, the average curve, with intermediary behavior that could be representative of the other two curves of the group.

In the composites CPA1.5A2.5C, CPA1.5A3.5C and CPM1A1C, due to distinct performances of the three curves of each group, it was selected instead of the average curve, the curve of higher potential to represent these composites. The potential curve is represents the behavior of exemplar which demonstrated higher ductility and resistance.

In the Figure [4] are presented the P-CMOD average curves for composite cement-based of mortar and microconcrete, respectively. The uneven behavior between the curves increased even more remarkably after the matrix rupture, i.e., when the contribution of fibers became more effective. The increase in the volume of fibers A provided a gradual improvement in the ductility of these composites. Considerably, the incorporation of microfibers C into fibers A contributed even more.

2.3.3 Fracture resistance curves

The curves of resistance obtained for the mortar composites CPA1.5A1.5C and CPA1.5A2.5C are compared with the curve of micro concrete CPM1A2C in the Figure [5], where K_R is the fracture resistance and α is the crack depth (a) relatively normalized at the height (W) of the prismatic specimen, i.e., α = a/W. In the figure are also represented the curves of resistance for the mortar and micro concrete with fibers together with the history of loading throughout the process of rupture.

As shown in Figure [5], from the point where begins the growth process of cracks in the matrix for the composites CPA1.5A1.5C, CPA1.5A2.5C and CPM1A2C, it is observed an eminent increase of resistance to fracture of these materials. For example, analyzing the top of crack at 70% from the section height, it is inferred that the fracture resistance reaches values up to four times higher than verified at 1/3 from the section height.

The extraordinary gain in resistance of these three composites was approximately similar, with a slight superiority for the mortar composite CPA1.5A2.5C, followed by microconcrete CPM1A2C and CPA1.5A1.5C. The development of resistance gain to fracture occurred for each composite according two well defined stages: the cracking initial stage (before the yellow dashed line), where it was verified a slight increase of toughness to fracture, and the cracking final stage (after the yellow dashed line), where the fracture resistance increased more pronouncedly.

Figure 5 – Composites performance

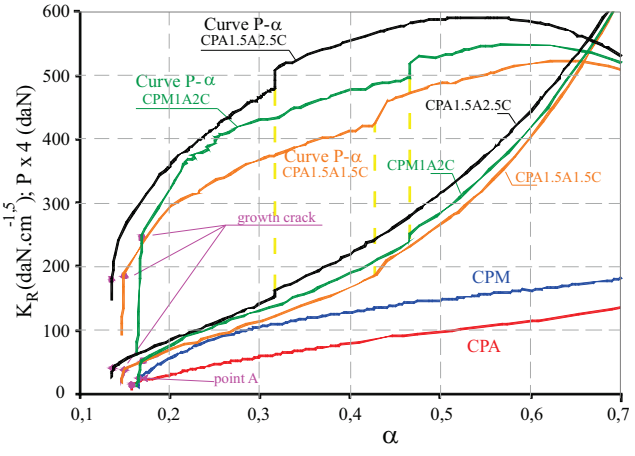

Table 3 – Characteristics of beams

Beams	Characteristics
V1A	RC beam. Without strengthening. Control
V1C	RC beam model strengthened by three layers of CFRPsheets
V2C	The tensile zone was demolished and retrofitting with high performance cement-based. RC beam model retrofitting and flexural strengthened by three layers of CFRP sheets

In the initial stage is where begins the tension process of steel fibers and microfibers and the stress transfer among the crack surfaces through these fibers. In this stage, in which occurs the formation of the cracks surfaces, it is observed that the crack develops more than the material gain resistance to fracture. In the last stage of the cracking process is when it is verified a considerable increase in fracture resistance for the composite due to the pulling out of fibers, which are anchored to the cement matrix. At this stage, the efficiency of fibers in relation to the contribution for the increase of fracture toughness is notably reflected.

3. Retrofitting and strengthening of tensile zone of RC beams

3.1 Characteristics of the beams

Three RC beams 3600 mm long were tested. All the specimens were designed to have the same nominal cross sectional dimensions: 170 mm x 350 mm. The lower longitudinal reinforcement of beams consisted of two steel bars CA50, with 12.5 mm diameter. The upper reinforcement was composed of two steel bars CA50, with 6.3 mm diameter. The transverse reinforcement was formed by stirrups with steel bars CA50 of 6.3 mm diameter, evenly spaced at every 120 mm. The characteristics of each beam are described in Table 3.

The beam V1A without strengthening was used as reference. From this reference were established considerations related to increment of resistance and stiffness provided by the strengthening. The beam V1A was designed with a reduced rate of longitudinal reinforcement so that its final limit state is characterized by the excessive deformation of reinforcement without rupture in the compressive concrete.

The beam V1C was flexural strengthened through the application of three sheet layers of carbon fibers. The strengthening was designed with the intent to detect its premature detachment. The beam V2C was designed to compare directly its performance with that of the strengthened RC beam. This comparison aims to detect the contributions of the transition layer before detachment and on the strengthening performance. For this purpose, the tensile zone of beam V2C was demolished and subsequently reconstructed by applying high performance cement-based composite CPM1A2C (Figure [6]). The composite CPM1A2C was by presenting a satisfactory performance in terms of flexural strength and fracture resis-

Figure 6 – Schematic of the beam V2C

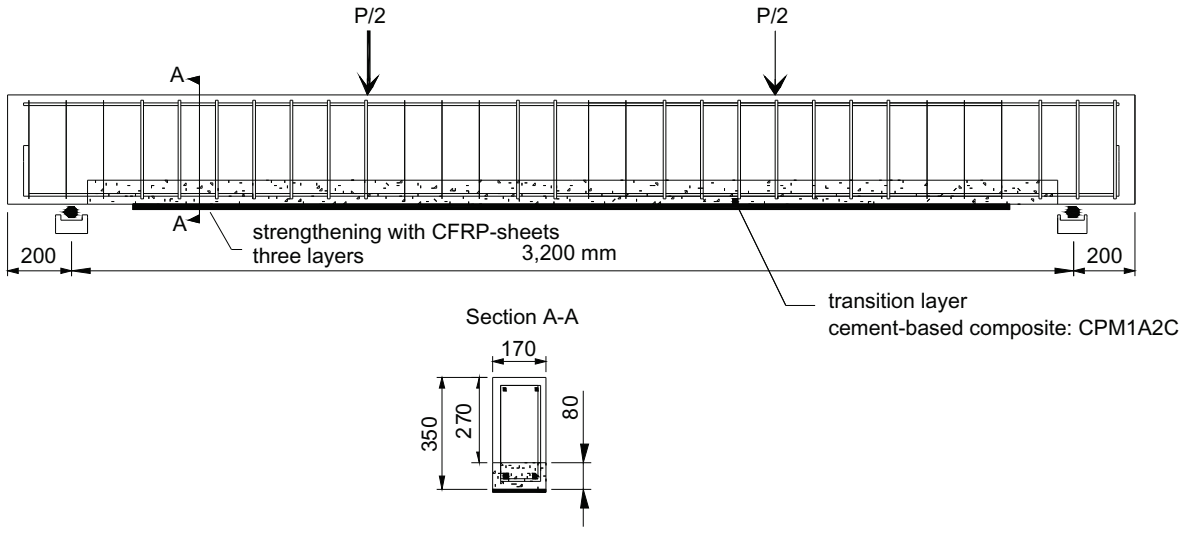

Figure 7 – Removal of concrete from the tensile zone of the beam V2C

tance. Further information on the development of composites can be found in Ferrari [6] and Ferrari & Hanai [9].

3.2. Retrofitting of tensile zone and application of strengthening on beams

The procedures to remove concrete, retrofitting and strengthening of tensile zone of beam V2C were initiated when the concrete had 23 days. The concrete removal was mechanically performed with electric breaker hammer and concluded with a sledgehammer, pointer and chisel Figure [7]. To prepare the tensile zone with composite CP-M1A2C, two molds of plasticized plywood were positioned on the two sides of the beam. The composite was manually placed into the molds. The general methodology used for the application of strengthening with steel fibers on the beams V1C and V2C are detailed in Ferrari [5]. The epoxy adhesive used was Sikadur 330 and the sheet was SikaWrap 300C, both, provided by Sika (Table [4]). The Figure 8 shows the layer aspect after its reconstitution and the strengthening.

3.3 Testing procedures

The RC beams were carried to a simple flexural at four points, through monotonic loading. The structural behavior of beams was observed and monitored throughout the test, recording the load, the corresponding vertical displacements and deformations of concrete, steel and strengthening.

The test setup was mounted on the plate reactor of the Laboratory of Structures of Engineering School of São Carlos (Figure [9]). The load to request each beam at flexion was introduced through an hydraulic actuator with 500 kN of nominal capacity, able to control

Figure 8 – Tensile layer aspect after the retrofitting and strengthening

Table 4 – Properties of the CFRP

	Comercial name	Sikadur 330
Epoxi adhesive	Colour	Part A – white / Part B – gray
	Tensile strength	30MPa (7 days)
	Tensile strain	9‰
	Bending modulus	3,800 MPa
	Tensile modulus	4,500 MPa
	Moisture	4:1 – A:B (weight)
	Consumption	1.0 a 1.5kg/m^2
Carbon fibers sheet	Comercial name	SikaWrap – 300C
	Weight	300g/m^2 ± 15g/m^2
	Thickness	0.166mm
	Density	1.79g/cm^3
	Tensile strength	3,900 MPa
	Elastic modulus	230 GPa
	Failure strain	15‰

the intensity and the application speed of loads and displacements. The beams were subjected to displacement-control of the actuator piston with the imposition of a rate of 0.007 mm/s. The actuator remained attached to a metallic beam of great stiffness, part of a reaction porch at the beam center. Strain gauges were attached to the steel reinforcements and strengthening to obtain strain profile. A data logger was used to read and record the values given by the strain gauges, load cells and linear variable displacement transducers (LVDTs). The nomenclature and scheme for positioning the instrumentation of beams are indicated in Figure [10].

Figure 9 – Schematic of the flexural test of beams

4. Test results

4.1 Failure modes

As expected, the mode of failure of the beam V1A was of excessive deformation for the longitudinal reinforcement, followed by high deformations in the compressive concrete.

The failure of the beam V1C (Fig. 11-a) began from the appearance of a crack at the strengthening end (P=117 kN). The propagation of this crack developed in horizontal direction and strengthening debonding with the entire layer of concrete from the reinforcement cover along the shearing span.

The mode of failure of the beam V2C (Figure [11-b]) was different from the observed for the beam V1C. Although it has appeared a crack at the strengthening end when the applied strength was 141 kN, it did not propagated horizontally and the debonding process for the strengthening by the rupture of concrete layer was avoided. In the beam V2C the failure was originated from a section located in the shearing span and near to the application of concentrated load. The appearance of a flexural/shearing crack and the development of its opening with the increment of load, cause the strengthening debonding through the cement composite interface with the epoxy adhesive until its nearest end. A thin layer of microconcrete remained jointed to the sheet.

Figure 10 – Nomenclature and positioning of the strain gauges and LVDT´S

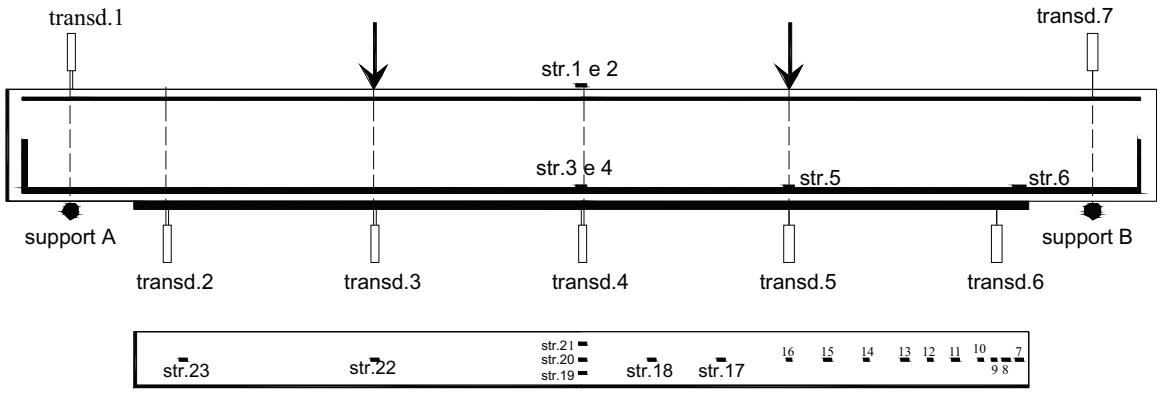

Strain gauges locations:

Strain gauges in the concrete and reinforcement

reference	number of strain gauge					
support A	1	2	3	4	5	6
0.0 mm	1600	1600	1600	1600	2250	2970

transd. = transductor
str. = strain gauge

Strain gauges in the strengthening

reference	number of strain gauge																
support A	7	8	9	10	11	12	13	14	15	16	17	18	19	20	21	22	23
0.0 mm	2970	2930	2890	2850	2770	2690	2610	2490	2370	2250	2034	1818	1600	1600	1600	950	350

4.2 Loads

In the Table [5] are showed the values of cracking load (P_f), of longitudinal reinforcement yield load (P_y) and beams failure load (P_u). The presence of strengthening increased the first crack load of the strengthened beams. The increment was of 19.8% for strengthened RC beam and 66.2% for the beam V2C. In relation to the beam V1C, the cracking load of beam V2C was increased by 38.8%.

The presence of strengthening increased also the load necessary for the longitudinal reinforcement yield. This occurs because the

Figure 11 – Failure modes of beams V1C and V2C

Table 5 – Loads and failure modes of the beams

Beams	P_f (kN)	P_y (kN)	P_u (kN)	Failure mode	Increments (%)		
					P_f	P_y	P_u
V1A	21.01	79.80	89.27	Excessive deformation for the longitudinal reinforcement	-	-	-
V1C	25.16	118.45	147.37	Strengthening debonding	19.8	48.4	65.1
V2C	34.92	133.37	196.35	Strengthening debonding through the cement composite interface	66.2	67.1	120.0

strengthening assists the steel to resist to tensile stresses. For the beam V1C the increase was of 48.4%. In the beam V2C the increase reached 67,1%.

Regarding the ultimate load it is highlighted the beam V2C response. A significant increment of 120% was observed in relation to the control beam, while the beam V1C presented a limited increment of 65.1%. Considering the strengthened RC beam, the resistance capacity for the beam V2C was 33.2% higher.

4.3 Vertical displacements

In the Figure [12] are compared, through the load-deflection curves (P-d), the behaviors for the beams V1A, V1C and V2C. It was observed that until the load cracking the response of beams is similar. After the concrete cracking, it is clear the increase of stiffness in the strengthened beams in relation to the beam without strengthening. It is emphasized the effect of the transition layer in the responses of the beam V2C. Higher stiffness and load capacity were verified for this beam, especially in relation to the beam of reinforced concrete V1C.

In the beam V1A it is observed that any addition of load after the yield of longitudinal reinforcement was obtained. As for the strengthened beams, it is clearly observed an increase of load after the longitudinal reinforcement yield. In this way, the largest extension for the final stretch of the curve of beam V2C indicates that the strengthening was more required in this beam than in the beam V1C.

In the Table [6] is presented a comparison between the deflection for beams in the middle of span for a load equal to 90% of the failure load of the beam V1A. The values show that the strengthened beams were stiffer than the control beam. The deflection of the beam V1A was 47% larger than the deflection of the beam V1C. The beam V2C presented a deflection even less pronounced than the beam without strengthening. The displacement of beam V1A was 67% higher than the beam V2C. Therefore, the innovation proposed in the present paper, retrofitting and strengthening of beam tensile zone, is not only effective in terms of load capacity, but also in terms of stiffness.

Figure 12 – Load-deflection curves of the beams V1A, V1C and V2C

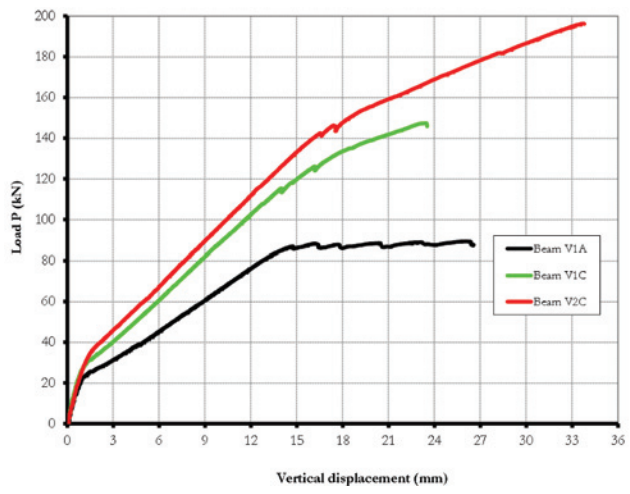

4.4 Stresses and strains

The strengthening response is evaluated through the distribution of specific strain throughout its extension. Associating the strengthening geometric and mechanical properties to values of strain it is possible to obtain a distribution of longitudinal and tangential stresses along the strengthening. It is possible to calculate

Table 6 – Comparative of beams deflections

Beams	Deflection (mm)	Comparison
V1A	12.79	1.00
V1C	8.73	1.47
V2C	7.68	1.67

the tangential stresses for the strengthening, among instrumented points, using the eq. 1.

$$\tau_r = \frac{\varepsilon_{r(i+1)} - \varepsilon_{r(i)}}{s_{(i+1)} - s_{(i)}} \cdot E_r \cdot t_r \quad (1)$$

where:
τ_r = is the tangential stress;
ε_r = is the strain in the strengthening;
s_i = relative position of the extensometer;
E_r = modulus of the strengthening;
t_r = thickness of the strengthening.

In the Figures [13] and [14] are presented the profiles of normal and tangential stresses along the strengthening of the beams V1C and V2C, respectively, for loads of 25%, 50%, 75% and 100% of the ultimate load. From the general analysis of these figures it is possible to verify that the maximum values of normal stresses were recorded in the central region of the beams. In the beams V1C and V2C the maximum value of normal stresses occurred at 213 mm of the middle of span and was recorded through strain gauge 18. On the other hand, a general examination of tangential stresses points out that the maximum values occurred in the region of the shearing span. With the increase of applied load to the beams, it is verified that the maximum values of tangential stresses tend to dislocate in the direction to the strengthening end. In the beam V2C, up to 50% for the failure load, the maximum value of tan-

Figure 13 – Distribution of normal and tangential stresses in the beam V1C

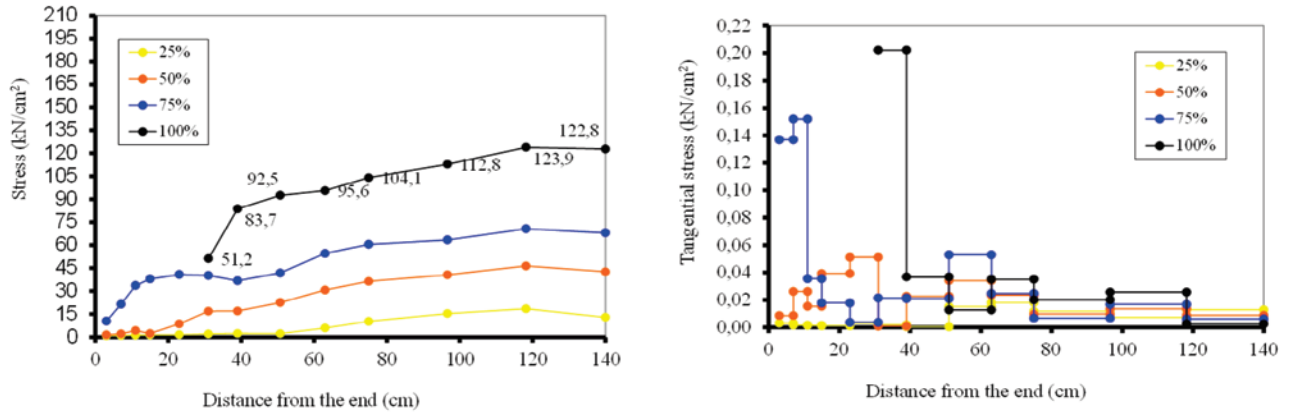

A normal stress

B tangential stress

Figure 14 – Distribution of normal and tangential stresses in the beam V2C

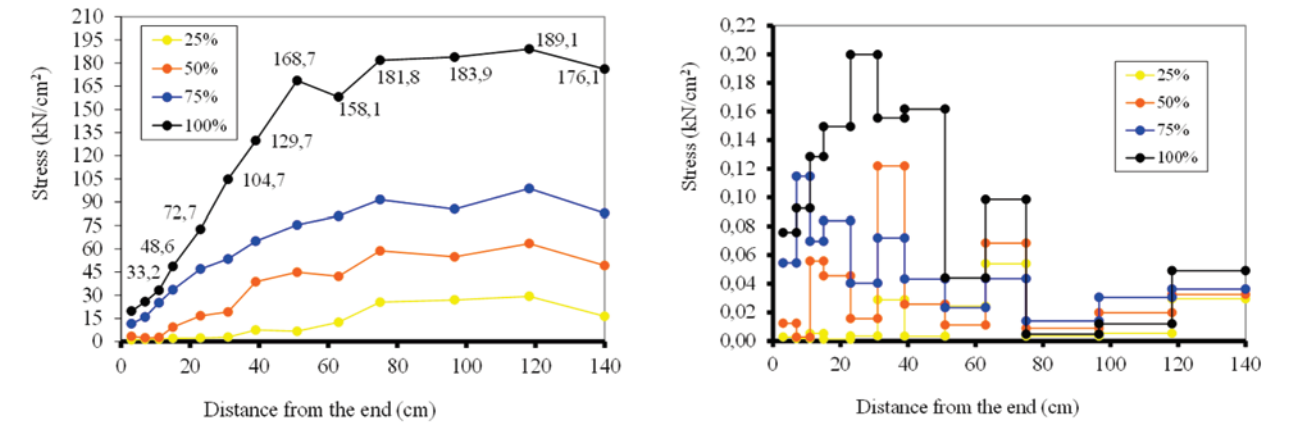

A normal stress

B tangential stress

Figura 15 – Malha de elementos finitos e disposição das armaduras

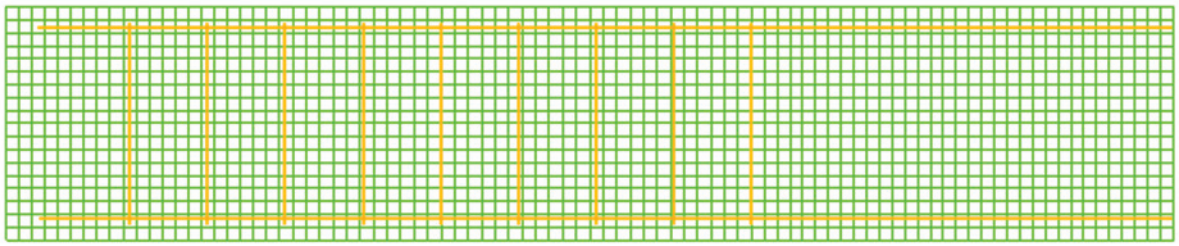

gential stress is located at 310 mm from the strengthening end. For the beam V1C this position was observed at 230 mm from the strengthening end.

In the beam V1C, the maximum normal stress, 1239 MPa, was recorded through the strain gauge 18, located at 218 mm from the section in the middle of span. This value of stress is equivalent to a deformation in the strengthening equal to 5.30‰. From the profile of stresses there are the verifications of significant values of normal stresses (in the order of 450 MPa) and the concentration of higher values of tangential stresses in the strengthening end at 75% and 100% from the last strength.

In the beam V2C the distribution of normal and tangential stresses along the strengthening (Figure [14]) indicates maximum values of 1891 MPa and 2 MPa, respectively. The maximum normal stress, which is equivalent to a strain in the strengthening of 8.08‰, was recorded by the strain gauge 18 and the maximum tangential stress was given by the strain gauge 11.

5. Finite element method (FEM) analyses

5.1 Discretization

The behaviors of beams V1A, V1C and V2C were nonlinearly simulated using the computational program of finite elements, Diana version 9.1. In the Figure [15], it is presented the mesh of two dimensional finite elements along with the arrangement of the reinforcements in the discretization of the beams. The mesh was developed using quadratic elements of 8-node type CQ16M. The longitudinal and transversal bars of the reinforcement of beams were discretely modeled through special elements called embedded reinforcement.

In the Figure [16] it is showed the loading application, the support, the presence of external strengthening, and the condition of model symmetry. The bond between the reinforcement and concrete was considered perfect, eliminating thus the possibility of rupture by slippage of the bars. The nodes of finite elements, representative of the external strengthening, were connected with the adjacent nodes of the concrete elements simulating a perfect bond between the materials.

The constitutive models of concrete beams considered in the program Diana and the mechanical properties of concrete and lower reinforcement used in the nonlinear analysis of the main beams V1A, V1C and V2C are listed in the Table [7]. These properties were obtained through characterization tests described in Ferrari [5].

The values of tensile strength considered for concrete, were those obtained according to ACI [10] through the equation: $0.332\times(f_c)^{1/2}$. The values of crack bandwidth were taken considering the square root of the finite element area, according to the recommendation in the Diana [11].

The presence of the transition layer in the beam V2C was established through a plane surface located in the tensile zone of the model. The bond between the transition layer and the surface representative of the adjacent concrete was considered perfect. The mechanical properties of the transition layer of beam V2C were taken from the characterization values of the cement composite and are indicated in the Table [8].

The values of tensile strength assumed for the cement composite were obtained through RILEM TC 162-TDF [8] using the equa-

Figure 16 – Contour conditions and concentrated load

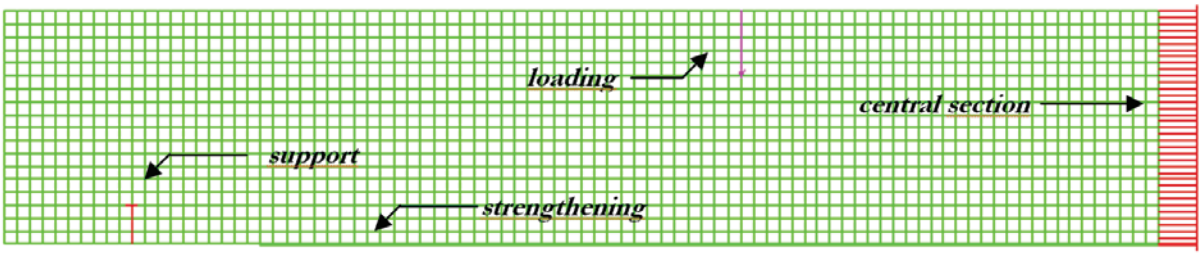

Table 7 – Materials and parameters for the numerical model of the beams V1A, V1C and V2C

	Parameters	Beams		
		V1A	V1C	V2C
Concrete	Elastic modulus	30,034 MPa	26,553 MPa	29,380 MPa
	Poisson's ratio	0.20	0.20	0.20
	Tensile strength	2.04 MPa	1.93 MPa	2.06 MPa
	Fracture energy	0.151 N/mm	0.123 N/mm	0.155 N/mm
	Width of the crack band	19.61 mm	20.12 mm	20.03 mm
	Compression strength	37.84 MPa	33.95 MPa	38.68 MPa
	Tensile behavior	Exponential model		
Steel	Elastic modulus	210,921 MPa	199,677 MPa	210,921 MPa
	Yield stress	547.99 MPa	532.44 MPa	547.99 MPa
	Behavior after yield	Elastic-perfectly plastic model		

tion: $0.6 \times f_{fct,L}$. The post-peak behavior of the cement composite was represented by an Exponential softening in tension diagram, having in the high value attributed to the energy of fracturing, the indication of the presence of fibers and microfibers of steel. The energy of fracture was calculated up to a deflection for the prismatic specimen, equal to d = 2.65 mm.

5.2 Numerical analysis results

In the Figure [17] the curves load-deflection numerically obtained are compared with the experimental results. Of the Figure [17-a] it is observed that in the elastic phase, the numerical curve for the control beam is identical to the experimental and after the concrete cracking, the numerical is stiffer.

For the control beam, the first crack load obtained numerically is 24.6 kN, which is 17% higher than the load 21.01 kN, of first crack, extracted from the experimental results. With the load of 85.3 kN, it occurs the reinforcement yield, represented by the sharp drop of stiffness of the numerical curve. This value exceeds the obtained experimentally (79.80 kN) only in 6.89%.

In the Fig. 18-b, it can be observed that the similar behavior of the numerical and experimental curves. After the concrete cracking and up to the load of 75 kN, the numerical curve is slightly more stiffen than the experimental. After this strength value, the curves develop again very similarly up to approximately 128.62 kN, and then up to the failure, the numerical curve develops with a stiffness lower than the experimental curve.

The first concrete crack obtained through the FE occurred with load equal to 26.96 kN, being this value 7.15% higher than the obtained experimentally. The reinforcement yield, according to the numerical model was given by a load of 122.4 kN, i.e., only 3.33% above the experimental value which is 118.45 kN. In addition, the load value corresponding to the failure pointed by the numerical model is 134.34 kN, while the experimental is 147.37 kN.

The Figure [18-c] shows that until the reinforcement yield, the numerical curve shows a higher stiffness than the experimental curve. After the reinforcement yield, the numerical curve begins to show higher values of vertical displacements than the experimental curve, within a same level of loading.

The first crack appearance according to the experimental results was given by the load of 34.92 kN, while by the numerical model was given by a load of 32.16 kN. The reinforcement yield according

Table 8 – Materials and parameters referring to the transition layer of the beam V2C

Numerical model V2C – Composite cement-based CPM1A2C
Linear Elasticity Isotropic, Young´s modulus = 28,700 MPa, Poisson´s ratio = 0.20
Static Nonlinearity Concrete and Brittle Materials, Total Strain Rotating Crack, Direct Input, Exponential Softening in Tension, Ideal in compression, Tensile strength = 2.24 MPa, Mode-I tensile fracture energy = 0.526 N.mm/mm^2, Crack bandwidth = (finite element area)$^{0.5}$ = 20.03 mm, Compressive strength = 28.07 MPa.

Figure 17 – Comparison between numerical and experimental curves load-deflection

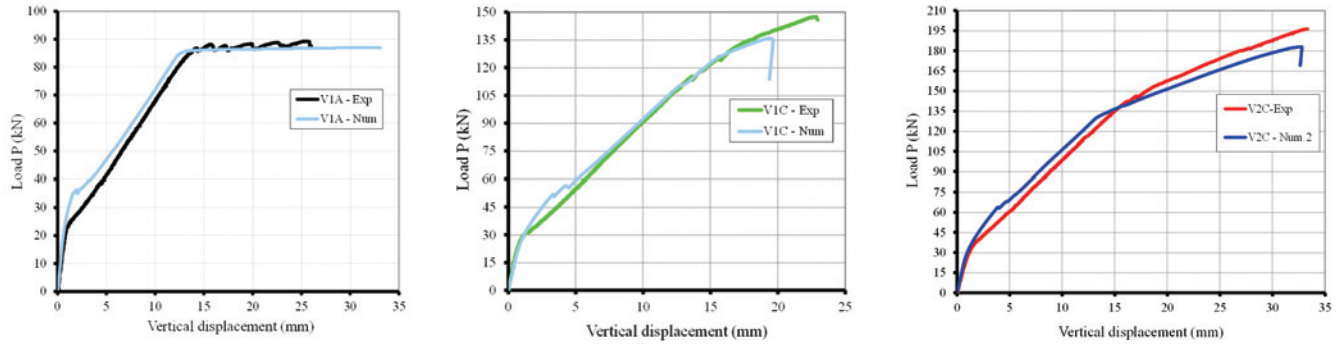

A Beam V1A B Beam V1C C Beam V2C

to the experimental results occurred at a load of 133.37 kN, while the numerical model indicated a yield at 129.64 kN. This value is 2.88% lower than the obtained experimentally. As for the failure of the beam V2C, the numerical model indicated a value of load of 182.9 kN, while the experimental value was 196.35 kN.

In general, the numerical curves of load-deflection for the control beam and strengthened beams presented a good concordance with the experimental curves. In the elastic phase, the behavior of the beams was practically identical, except for the curve of model V2C, a little more rigid than the experimental curve, even in this phase of loading.

Until the reinforcement yield, the numerical curves showed more stiffness than the experimental curves. Additionally, after the reinforcement yield, the deflections represented by the models of the strengthened beams were more pronounced than the experimental results.

In the Figure [18] is illustrated the comparisons of development of strains in the strengthening obtained experimentally with the results extracted from the numerical analysis. The values of strain refer to the middle section of the beam. For the beam V1C, the values of numerical strains of the strengthening in the middle of span were highly correlated with the experimental values. Even after the concrete cracking and the reinforcement yield, the development of numerical strains represents satisfactorily the experimental values. Until the reinforcement yield, the numerical curve is slightly more inclined than the experimental curves. After the reinforcement yield, the numerical strains of strengthening develop more pronouncedly and thereafter the failure occurs.

In the Figure [18-b] it is observed that the numerical model reflects well the development of experimental strains in the strengthening of the beam V2C. Before the reinforcement yield, the numerical curve is more inclined than the experimental curve. Even after the reinforcement yield, the numerical curve develops similarly to the experimental strains.

6. Conclusions

This research aimed to propose and examine an innovative constructive technique for the flexural strengthening of RC beams.

Figure 18 – Numerical and experimental strains in the middle of the strengthening

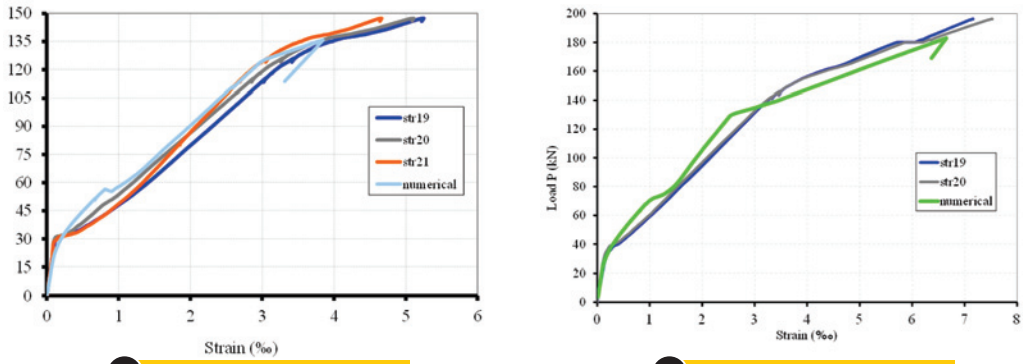

A Beam V1C B Beam V2C

This technique involves a process of previous retrofitting of beams with a high performance composite based on Portland cement and short steel fibers, intended to constitute the called transition layer. After the performance of several steps of experimental and theoretical analysis, it can be concluded that the technique proposed – even with the possibility of further improvements, as any other technique – proved to be efficient both in the reconstitution of tensile zone of RC beams and in the improvement of beam performance as a whole, particularly in a more efficient exploration of the resistance properties of strengthening with sheets of PRFC.

The research was not limited to simple testing and comparison of strengthened and non-strengthened beams, but aimed to cover several scientific foundations and evaluations that focused on the problem in question. From the joint analysis of all results obtained, it could be concluded that the intended objective was reached.

Finally, it is highlighted a synthesis of the partial conclusions and complementary comments on each specific study produced:

the addition of steel microfibers to conventional fibers enhances the contribution of the matrix to the composite resistance and the improvement in the mechanism of stress transfer from matrix to fibers; with the matrix cracking, the stress transfer was facilitated by the steel microfibers which, in large amount in the matrix, led to the progress of cracking with the increase in the loading level;

the flexural strengthening of beams through the external bonding of CFRP sheet to a transition layer constitutes an efficient strategy with practical application in engineering;

despite of being analyzed, during the last experimental steps, for a single case (beam V2C), it was demonstrated that the previous reconstitution of tensile zone with a high performance cement-based composite based on macro and microfibers of steel prevents the rapid progression of a critical crack at the strengthening end and delays the sheet premature detachment. In the presence of a material with greater fracture strength in the tensile zone of the beam, the cracks become more distributed and with small openings along the strengthening extent.

besides the considerable increase in resistance, the bonding of CFRP sheet to a transition layer leads to a significant increase of beam stiffness in relation to a beam without transition layer.

7. Acknowledgements

We thank FAPESP and CAPES for financial support. We also thank Maccaferri – Latin America for the production, under purchase order, of steel microfibers.

8. References

[01] Juvandes L. Strengthening and rehabilitation of concrete structures using composites materials. Thesis, Porto University Engineering; 1999.

[02] Ferrari VJ. Flexural strengthening of reinforced concrete beams with carbono fibers sheets. Thesis, Federal University of Santa Catarina; 2002.

[03] Beber, AJ. (2003). Structural behavior of strenghetened reinforced concrete beams with steel fibers composites. Thesis, Porto Alegre. Tese, Federal University of Rio Grande do Sul; 2003.

[04] FIB. Bond of reinforcement in concrete-state-of-the-art report. Lauseanne. Bulletin 10. 2000.

[05] Ferrari VJ. Flexural strengthening of reinforced concrete beams with carbon fibers reinforced polymer sheet bonded to a transition layer of high performance cement-based composite. Thesis, University of Sao Paulo, School of engineering; 2007.

[06] Ferreira LET. About the fracture resistance concrete and the steel fibers concrete. Thesis, University of Sao Paulo; 2002.

[07] RILEM TC 162-TDF. Test and design methods for steel fibre reinforced concrete. Bending test. Materials and Structures, 2002a; 35, 579-582.

[08] RILEM TC 162-TDF. Test and design methods for steel fibre reinforced concrete. Design of steel fibre reinforced concrete using the s-w method: principles and applications. Materials and Structures, 2002b; 35, 262-278.

[09] Ferrari, V.J; Hanai, J.B. Development and analysis of high performance hybrid cement composites. Ibracon Structures and Materials Journal, 2009; 3, 254-270.

[10] ACI.318M. Building code requirements for reinforced concrete.1989

[11] DIANA – Finite Element Analysis – user's manual release 9.